STUDY OF BEAM DYNAMICS IN LINEAR PAUL TRAPS

D.J. Kelliher, S. Machida, C.R. Prior, S.L Sheehy
STFC Rutherford Laboratory, ASTeC, UK.

Abstract

The Hamiltonian governing the dynamics in a Linear Paul Trap (LPT) is identical in form to that of a beam in a focusing channel. This similarity, together with the LPT's flexibility, compactness and low cost, make it a useful tool for the study of a wide range of accelerator physics topics. Existing work has focused on high intensity collective effects as well as, more recently, the study of integer resonance crossing in the low intensity regime. A natural extension of this work is to investigate space-charge effects of intense beams in more realistic lattices to directly inform accelerator design and development. For this purpose we propose to construct a modified Paul Trap specifically for these studies. Among other features, it is envisaged that this new LPT should be able to model non-linear elements and a wider range of lattice configurations. This work will be undertaken in collaboration with Hiroshimi University.

INTRODUCTION

In a linear Paul Trap ions are trapped transervsely by an oscillating RF field and axially by a static DC field. The use of such a device to study the transverse dynamics in a quadrupole channel was first proposed in ref. [1]. The equivalence between the two cases includes not only the Hamiltonian but also the Vlasov-Poisson equation [2]. It follows that the collective processes and transverse dynamics are identical in the two systems.

A LPT allows the study of beam dynamics in a relatively cheap and compact device. It also allows more flexibility in the choice of parameters (e.g. radio-activation by beam loss does not apply). The time allocated to study accelerator physics on production machines is normally limited - this is not an issue in an ion trap.

A wide range of beam dynamics experiments have already been conducted in LPTs including the study of collective modes [3,4], the crossing of parametric resonances [5], the role of noise in emittance growth and halo production [6,7], the adiabatic compression of a bunch [7] and resonance instability bands in doublet lattices [8].

Experiments to date have been done either on the Paul Trap Simulator Experiment (PTSX) device at Princeton, USA or on the Simulator of Particle Orbit Dynamics (S-POD) series of traps at Hiroshima, Japan. It is proposed to construct a new trap (or series of traps) at Rutherford Appleton Laboratory, UK. This will be done in close collaboration with the Hiroshima group.

While there is certainly much more that could be done using existing traps, it is worth investigating the broader range of experiments that might be made possible with modified designs. Here we consider a multipole trap to allow non-linear lattices to be studied. In the next section the essential formulae that inform the choice of the principal trap parameters are given. In later sections, collective effects, halo production, detuning and the flexibility in lattice choice are covered.

LPT DESIGN

In the original "3D" Paul trap, the RF field is zero at just a single point at the centre of the device thus limiting the number of ions that can be cooled. By contrast a "linear" quadrupole field allows a string of ions to be cooled along the axis, hence the development of the linear Paul trap (also called a "linear quadrupole trap"). This device can be generalised to the "linear multipole trap" (henceforth referred to as a multipole trap) in which additional electrodes add non-linear field components [9].

For the case of a linear quadrupole trap, we follow the analysis in ref. [10], which starts with the envelope equation for each transverse plane. Throughout this paper we use x and y to refer to the two transverse coordinates and z for the axial coordinate. In the horizontal case, assuming an rms radius a and applying the smooth approximation, the equation is

$$\frac{d^2a}{d\tau^2} + \kappa^2 a - \frac{\epsilon_x^2}{a^3} = \frac{Nr_P}{2a} \qquad (1)$$

where $r_p = q^2/4\pi\varepsilon mc^2$ is the classical particle radius, N is the line density, κ is a focusing constant and $\tau = ct$ and ϵ_x is the horizontal emittance given by

$$\epsilon_x = \frac{1}{mc}\sqrt{\langle x^2\rangle\langle p_x^2\rangle - \langle xp_x\rangle^2} \qquad (2)$$

A similar equation applies in the vertical plane. The vacuum phase advance per RF oscillation σ_0 (equivalent to the phase advance per cell in an accelerator lattice) is defined as

$$\sigma_0 \equiv \kappa c/f = \frac{2\sqrt{2}qgV_0}{\pi^2 m}\left(\frac{1}{fR}\right)^2 \qquad (3)$$

where f is the RF frequency, R is the radius of the trap, V_0 is the amplitude of the RF waveform applied to the electrodes and g is a shape function defined in [10]. Note - the transverse oscillation frequency ω_0, which will be useful later, is given by $f\sigma_0$ and the transverse tune ν_0 is $2\pi\sigma_0$. Assuming a stationary plasma ($\frac{d^2a}{d\tau^2} = 0$) and defining the transverse temperature $T_\perp$ to be

$$k_BT_\perp = \frac{\langle p_x^2\rangle}{m} \qquad (4)$$

where k_B is the Boltzmann constant. One obtains

$$N = \frac{2}{r_P}\left[\sigma_0^2\left(\frac{af}{c}\right)^2 - \frac{k_BT_\perp}{mc^2}\right] \qquad (5)$$

Equation (3) can be rearranged in terms of RF frequency

$$f = \frac{1}{\pi R} \sqrt{\frac{2\sqrt{2}q}{m} \frac{V_0 g}{\sigma_0}} \qquad (6)$$

and by substituting a σ_0 term in Eqn. (5) with Eqn. (3) yields the following

$$N = \frac{8\pi\epsilon}{q^2} \left[\frac{2\sqrt{2}g\alpha^2}{\pi^2} qV_0\sigma_0 - k_B T_\perp \right] \qquad (7)$$

where $\alpha = a/R$ ($0 < \alpha < 1$). By arranging the equation for the line density in this way, it is made clear that it is proportional to V_0 for any fixed phase advance.

Table 1: PTSX and S-POD Trap Parameters

Parameter	PTSX	S-POD
Length (m)	2.0	0.1
Radius (m)	0.1	0.005
Max voltage (V)	235	100
RF frequency (MHz)	0.075	1.0
Plasma radius (m)	~ 0.01	~ 0.001
Ion species	Cs-133, Ba-137	Ar-40, Ca-40

From Eqn. 1 it can be shown that the depressed transverse oscillation frequency ω is given by

$$\omega^2 = \omega_0^2 - \frac{\omega_p^2}{2} \qquad (8)$$

where ω_0 is the frequency in the zero intensity limit and $\omega_p = \sqrt{Nr_p c^2/a^2}$ is the plasma frequency (here we assumed the plasma density is uniform). The normalised tune depression η is then given by

$$\eta \equiv \frac{\nu}{\nu_0} = \frac{\omega}{\omega_0} \qquad (9)$$

In the space-charge limit $\omega_p \to \sqrt{2}\omega_0$ and $\eta \to 0$. Recalling that the phase advance is given by ω/f then Eqn. (8) becomes

$$\sigma^2 = \sigma_0^2 - \frac{Nr_p}{2} \left(\frac{c}{fa} \right)^2 \qquad (10)$$

Using Eqn. (5), the above can be rewritten in terms of η

$$\eta = \sqrt{1 - \frac{1}{1 + (2/Nr_p)(k_B T_\perp/mc^2)}} \qquad (11)$$

Note, η is independent of the mass of the ion species since $r_p \propto 1/m$. By cooling the plasma (using laser cooling techniques) towards absolute zero one can achieve $\eta \sim 0$ at which point the plasma enters a crysalline state (Coulomb crystal).

The main parameters to choose when designing a LPT are the frequency and voltage to apply to the electrodes, the trap radius and length and the choice of ion species. The
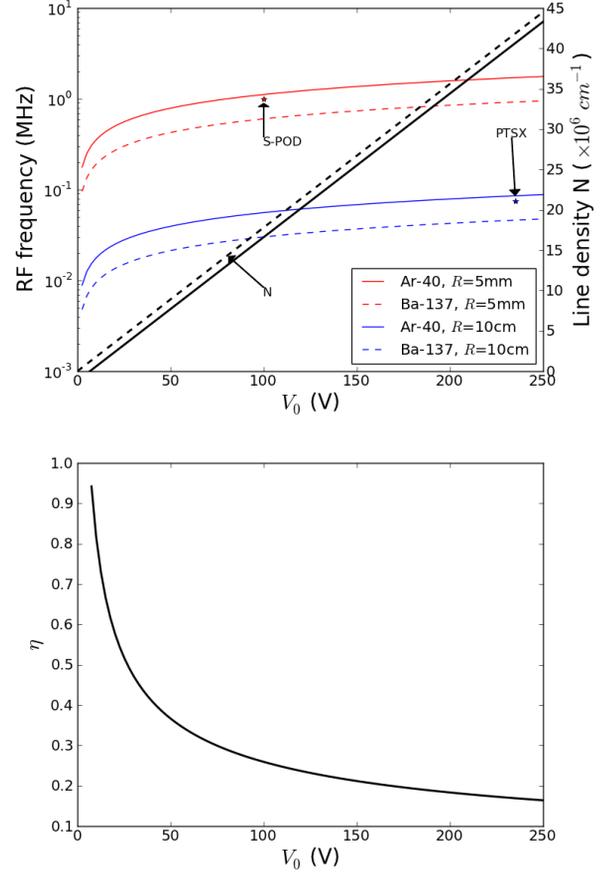
Figure 1: Top: Estimated line density and required RF frequency as a function of peak voltage V_0 for a stationary plasma with the phase advance set at $\pi/2$ in Eqns. (6, 7). The line density is shown with the temperature set to 1000 K (solid black line) and 0 K (dash black line). The RF frequency is shown for the case of Ar-40 and Ba-137 ions when the radius R is 5 mm (red) and 10 cm (blue). The actual RF frequency and peak voltage employed by S-POD and PTSX are also indicated. The shape function $g \approx 0.712$ and $\alpha = 0.2$ have been assumed as in ref. [10]. Bottom: Normalised tune depression η obtained from Eqn. (11), making use of the line density in upper figure, and assuming the temperature is 1000 K. At 0 K it is trivially equal to zero.

line density (and hence η) for a particular phase advance is given by the voltage and temperature (Eqn. (5, 11)). Once the voltage is chosen, the product of the RF frequency and the trap radius is a constant (Eqn. (6)).

This is illustrated in Fig 1 which shows the RF frequency versus voltage when the trap radius is 5 mm and 10 cm, corresponding to the radii of S-POD and PTSX, respectively. The principal parameters of these traps given in Table. 1. As can be seen in the table a substantially lower RF frequency is needed at the higher radius but at the expense of a much longer trap (the required length roughly scales with the radius to ensure end effects can be neglected). It is also apparent that very low values of η (in accelerator terms)

COLLECTIVE MODES

Sacherer found that coherent resonance condition is satisfied when the tune of a collective mode Ω_m is integer [11]. In terms of incoherent tune shift the resonance condition becomes

$$\nu_0 - C_m \Delta\nu \approx \frac{n}{m} \qquad (12)$$

where ν_0 is the bare tune, $\Delta\nu$ is the incoherent tune shift induced by space-charge and C_m is a coherent mode coefficient which is less than unity for every mode [12]. It was later found [13] that resonances may also be driven at $\Omega_m \approx n/2$ which leads to

$$\nu_0 - C_m \Delta\nu \approx \frac{n}{2m} \qquad (13)$$

The above implies the existence of a space-charge driven resonance at a quarter integer for the $m = 2$ mode. This resonance (among others) has been identified in LPT experiments in which both the stopband was measured [3] and the resonance crossed [5].

Direct detection of a collective mode can be made by measuring the signal it produces. It may not be feasible to detect the typically small perturbation voltage induced on the main electrodes. A separate capacitive pickup electrode was installed in one LPT in order to measure the collective mode signal [14]. This consisted of azimuthally segmented ring electrodes placed inside the main confining electrodes. The segmentation allows the discrimination of different azimuthal mode numbers. The radius of the electrode was carefully selected to allow the signal to be detected while not intercepting the plasma. Using this diagnostic the axisymmetric body-wave mode and quadrupolar surface mode were detected [14].

It is of interest to study how space-charge induced resonances can be enhanced or mitigated by applying nonlinear fields. In fact emittance growth and beam loss is often caused by chaotic motion near non-linear resonances which can be driven either by space-charge effects and/or non-linear elements [15]. An octupole introduces an amplitude dependent tune spread which can damp the effect of resonances [16]. For this study a multipole trap would be required.

Instabilites arising from various self-forces of a bunch are mainly of particular interest in cases where the space-charge is high (e.g. in high intensity linacs). Emittance exchange driven by the self-field of the perturbed bunch can lead to harmful instabilities. Assuming the unperturbed bunch has uniform density within the elliptic cross section defined by

$$\left(\frac{x}{a}\right)^2 + \left(\frac{y}{b}\right)^2 \leq 1 \qquad (14)$$

we may write, assuming the smooth approximation, the transverse emittance ratio ϵ_x/ϵ_y as follows

$$\frac{\epsilon_x}{\epsilon_y} = \frac{a^2 \nu_x}{b^2 \nu_y} \qquad (15)$$

and the energy (temperature) anistropy τ as

$$\tau = \frac{\epsilon_x \nu_x}{\epsilon_y \nu_y} \qquad (16)$$

for tunes ν_x, ν_y.

Dispersion relations for modes of various order are given in terms of these dimensionless parameters in ref. [17]. It is found that, in some cases and in certain parameter regimes, stable modes for round isotropic beams ($a/b = 1$, $\tau = 1$) become unstable in the anisotropic case. For example, the second order odd (tilting) mode is unstable for a sufficiently large anisotropy.

Although ref. [17] deals with anisotropy between the horizontal and vertical planes, the same results apply for the transverse and longitudinal planes. For a particular choice of emittance ratio, regions of instability can be found in terms of the normalised radial depressed tune ν_r/ν_{r0} versus tune ratio ν_z/ν_r. These so-called "Hofmann Stability Charts" (Fig. 2 is an example) are widely used in the design of high intensity linacs. Experiments performed in linacs provide evidence of expected instabilities for certain values of temperature anisotropy [18].
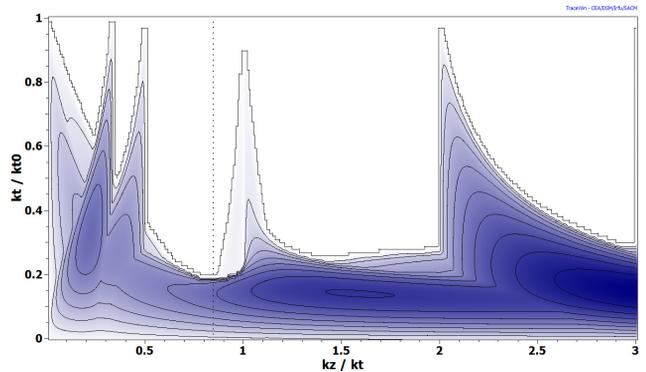
Figure 2: Example of a Hofmann Stability Chart for the emittance ratio $\epsilon_z/\epsilon_t = 1.2$ where z and t refer to the longitudinal and transverse planes, respectively. The vertical axis covers the full range of depressed tunes k_t/k_{t0} while the horizontal axis is the tune ratio k_z/k_t. The contours show low to high emittance exchange between the two planes in increasingly dark shades of blue. The vertical dotted line corresponds to equal temperatures in the two planes, $\tau = 1$. This figure is from ref. [18] provided courtesy of the authors.

The idea of studying emittance exchange in a LPT is under consideration. For a stationary plasma in a linear Paul trap, the temperature among the three degrees of freedom is approximately uniform $T_x = T_y = T_z$. In order to investigate equipartition, it is desired that a controlled level of temperature anisotropy is introduced. This can be done by cooling along one or more degrees of freedom. Using laser cooling directed along the z axis, the axial temperature T_z can be substantially reduced while the transverse temperature $T_\perp$ remains relatively unaffected.

HALO FORMATION

Halo formation was among the first beam dynamics topics to be suggested for study in ion traps [1]. In one study, by adding noise to the quadrupole electrodes for many oscillations of the confining RF the growth of a non-thermal tail of trapped ions was observed [6]. Halo formation has also been observed in a Penning trap [19]. Evidence for halo formation can be found by extracting the ion plasma and measuring the charge as a function of radius using a multi-channel or transverely moveable Faraday Cup [1, 6] (or phosphor plate imaged by CCD camera). In modern high intensity accelerators, beam loss may be even lower than the 1% level [20]. It follows that diagnostics used on the LPT should have sufficient resolution to detect very small halo populations.

In recent years, studies of halo formation have concentrated on the interplay of space-charge forces, non-linear lattice elements (e.g. octupole) and synchrotron motion. Frozen core models have been developed which allow the particles outside the core to be treated separately from those within. The synchrotron motion modulates the tune via the uncorrected chromaticity, but also modulates the space-charge force in the transverse plane and hence the depressed betatron tune [21]. Since the synchrotron tune is much less than the betatron tune, the effect is an adiabatic modulation of transverse phase space [22]. Although longitudinal effects cannot be studied in a conventional LPT, the transverse phase space could be adiabatically modulated, for example by slowly varying the RF voltage of the quadrupole electrodes (and so the tune), to emulate this process.

In order to study halo formation in detail, and see evidence for effects such as scattering from or trapping in resonant islands and diffusion from chaotic regions, a real-time, high-resolution, non-destructive measurement of phase space would be invaluable. Such a measurement is in principle possible using the technique of laser-induced fluorescence (LIF) [23].

RESONANCE CROSSING AND DETUNING

One or more resonances can be crossed in a LPT and the effect on the number of trapped ions can be measured. As well as the space-charge induced resonances mentioned earlier, the crossing of integer tune resonances excited by dipole errors has also been studied [24]. The tune can be varied in a single experiment by varying either the voltage or frequency of the waveform applied to the confining electrodes (Eqn. (3)). A dipole error is introduced by applying an additional RF signal to one or two of the electrodes. This perturbation waveform should be a harmonic of the confining RF in order to create a stopband around a single integer only. Multiple integer resonances can be excited by perturbing with a superposition of harmonics.

Some of the results from the integer tune crossing study suggests the influence of high order multipoles [25]. Imperfections in the electrode construction and alignment results

in non-zero multipole components [10]. It would be interesting to carry out a resonance crossing study in a multipole trap to measure the effect of a controllable level of non-linearity.

If the tune is set to be exactly on an integer resonance, a dipole kick should cause the magnitude of coherent oscillations to grow without bound. Non-linearities may cause the tune to move away from the resonance via amplitude detuning. If the non-linearity is strong enough, or the dipole kick low enough, the growth of the centroid amplitude of the plasma will reach a plateau. It is predicted that in the case of linear amplitude detuning ($\nu = \nu_0 + \mu I$), the plateau should scale with $(F/\mu)^{1/3}$ where F is the magntitude of the dipole perturbation, I is the amplitude in μ the detuning coeficient [26]. Detuning with amplitude could be a topic for study in a multipole trap.

LATTICE FLEXIBILITY

Most beam dynamics studies to date have simulated FODO lattices since it can be implemented by simply applying a sinusoidal waveform to each electrode. Doublet, triplet and FFDD lattices have recently been created by adding waveforms with the appropriate structure [19]. Lattices with unequal tunes in the two transverse planes can also be realised by applying different pulse widths to each pair of electrodes. The dependence of space-charge resonances on the lattice configuration was investigated for the doublet case [8], a study that could be extended to other lattice configurations.

It would be of interest to implement the lattices of existing or planned accelerators for study in a LPT. A multipole trap would greater extend the reach of ion trap experiments by allowing non-linear elements to be included. The relative timing of the voltage pulses applied to the electrodes for each multipole order would allow the ordering of the "magnets" to be chosen.

For example, the field in a scaling FFAG varies with radius r according to $B = B_0(r/r_0)^k$ where k is the field index and B_0, r_0 are defined at some reference radius. Though this field profile contains multipoles of every order, it can be approximated by truncating around r_0 the multipole expansion of the field profile $B = \sum_n k!/(n!(k-n)!) * ((r-r0)/r0)^n$ (as was done for the PAMELA FFAG design [27]). The practicalities of trap design would need to be considered for a significant number of multipoles.

DISCUSSION

The potential for beam physics studies in LPTs would be greatly extended in traps with higher order multipoles and by the use of a non-destructive, in-situ diagnostic such as LIF. Pure multipole traps have already been constructed for the purpose of reducing rf heating (and so create a greater volume in which ions are cooled). However, as far as the authors know, no LPT in which more than one multipole may be individually set has yet been constructed.

A design for such a trap, with adjustable quadrupole and octupole electrodes is presented in [10]. Inside the main

confining quadrupole electrodes, sit four octupole electrodes with much smaller radii. Simulations confirm that the octupole component can be specified by sending a separate waveform to this set of electrodes. Further progress has recently been made on multipole trap designs [28].

Several practical difficulties are envisaged - including the screening of the potential from one set of electrodes by another, the effect of unwanted multipoles induced by imperfections in the electrode smoothness or alignment and the extra electronics and feedthrough cables required to feed ~MHz signals to many electrodes without reflections, and with the correct phase and amplitude.

ACKNOWLEDGMENT

REFERENCES

[1] H. Okamoto, H. Tanaka, Nucl. Instr. Meth. A 437, 178 (1999).

[2] R.C. Davidson, H. Qin and G. Shvets, Phys. Plasmas 7,1020 (2000).

[3] S. Ohtsubo et al., Phys. Rev. ST Accel. Beams 13, 044201 (2010).

[4] E. Gilson et al., Phys. Plasmas 20, 055706 (2013).

[5] H. Takeuchi et al., Phys. Rev. ST Accel. Beams 15, 074201 (2012).

[6] M. Chung et al., Phys. Rev. Lett. 102, 145003 (2009).

[7] E. Gilson et al., Phys. Plasmas 17, 056707 (2010).

[8] K. Fukushima et al., Nucl. Instr. Meth A 733, 18-24 (2014).

[9] F.G Major, V.N. Gheorghe, G. Werth, *Charged Particle Traps*, (Berlin: Springer, 2005), 109.

[10] H. Okamoto et al., Nucl. Instr. Meth A 485, 244-254 (2002).

[11] F.J. Sacherer, Ph.D thesis, Lawrence Radiation Laboratory [Report No. UCRL-18454].

[12] R. Baartman, Proc. of the Workshop on Space Charge Physics in High Intensity Hadron Rings (AIP, Shelter Island, 1998), p. 56.

[13] H. Okamoto, K. Yokoya, Nucl. Instr. Meth. A 482, 51 (2002).

[14] E. Gilson et al., Nucl. Instr. Meth A 606, 48-52 (2009).

[15] K. Ohmi, Proc. of IPAC13, Shanghai, China, 1589 (2013).

[16] A.V. Fedotov, J. Wie, V. Danilov, Proc. of IPAC13, Shanghai, China, 1589 (2013).

[17] I. Hofmann, Phys. Rev. E 57(4), 4713 (1998).

[18] C. Plostinar, M. Ikegami, Y. Liu, T. Maruta, Proc. of IPAC13, Shanghai, China, 3966 (2013).

[19] H. Okamoto et al., Proc of IPAC14, Dresden, Germany, 4056 (2014).

[20] H. Hotchi, Prog. Theor. Exp. Phys. 02B003 (2012).

[21] G. Franchetti et al., Phys. Rev. ST Accel. Beams 13, 114203 (2010).

[22] A. Bazzani et al., AIP Conf. Proc. 773, 158 (2005).

[23] M. Chung et al., Nucl. Instr. and Meth. A 544, 514-519 (2005).

[24] D.J. Kelliher et al., Proc of IPAC14, Dresden, Germany (2014).

[25] K. Moriya et al., Submitted for publication (2014).

[26] S.R. Mane and W.T. Weng, Nucl. Instr. Meth. A 306, 9-20 (1991).

[27] S.L. Sheehy et al, Phys. Rev. ST Accel. Beams 13, 040101 (2010).

[28] H. Okamoto, K. Fukushima, K. Ito, T. Okano, TUO2LR03, HB2014, these proceedings (2014).